ID Design 2012/DOOEL Skopje, Republic of Macedonia
South East European Journal of Immunology
Volume 2016; Article ID 20007, 8 pages
http://dx.doi.org/10.3889/seejim.2016.20007
Basic Immunology

ROS-mediated Cytotoxicity and Macrophage Activation Induced by TiO_2 Nanoparticles with Different *in vitro* Non-Cellular Photocatalytic Activities

Traian Popescu[1], Lidia Cremer[2], Mihaela Tudor[2], Andreea-Roxana Lupu[2,3*]

[1]National Institute of Materials Physics, P.O. Box MG-7, 077125, Bucharest, Romania; [2]Immunomodulation Group, "Cantacuzino" National Research Institute, Bucharest, Romania; [3]Immunobiology Laboratory, Assay Development and Alternative Testing Team, "Victor Babes" National Institute of Pathology, Bucharest, Romania

Citation: Popescu T, Cremer L, Tudor M, Lupu A-R. ROS-Mediated Cytotoxicity and Macrophage Activation Induced By TiO_2 Nanoparticles with Different *in Vitro* Non-Cellular Photocatalytic Activities. SEE J Immunol. 2016 Apr 19; 2016:20007. http://dx.doi.org/ 10.3889/seejim.2016.20007

Key words: TiO_2 nanoparticles; macrophages; reactive oxygen species; inflammation; IL-6.

[*]**Correspondence:** Andreea-Roxana Lupu. Immunomodulation Group, "Cantacuzino" National Research Institute, Bucharest, Romania. Tel: +40213192732. Email: immunomod@cantacuzino.ro, ldreea@gmail.com

Received: 31-Jan-2016; **Revised:** 08-Apr-2016; **Accepted:** 09-Apr-2016; **Published:** 19-Apr-2016

Competing Interests: The author have declared that no competing interests exist.

Abstract

AIM: The aim of the study described in the present paper was to assess several *in vitro* effects of TiO_2 nanoparticles with different colloidal and photocatalytic properties on RAW 264.7 macrophages.

METHODS: The cells were exposed to Degussa P25 titania and two other types of nanoparticles synthesized by a hydrothermal procedure in our laboratory: undoped and Fe^{3}+-doped TiO_2. Compared to Degussa P25, the hydrothermal nanomaterials were significantly less active in inducing cytotoxicity, production of intracellular reactive oxygen species (ROS) and release of pro-inflammatory cytokine interleukin-6 (IL-6). The induced effects were analysed with respect to nanoparticle size, surface charge, hydrophilicity, semiconductor bandgap energy and photocatalytic generation of ROS under non-cellular conditions.

RESULTS: The overall results indicated that TiO_2 nanoparticles with higher surface charge, hydrophilic surfaces and enhanced photocatalytic properties may preferentially induce macrophage cell damage and inflammation compared to other TiO_2 nanomaterials.

CONCLUSION: The present findings are relevant for studies regarding the evaluation of risks raised by self-cleaning technologies involving nanosized hydrophilic TiO_2 photocatalysts as well as development of synthesis methods optimized for producing biocompatible TiO_2 nanomaterials.

Introduction

Titanium dioxide (TiO_2, titania) is a multifunctional material with optical (high refractive index, absorption of ultraviolet (UV) radiation), photocatalytic [1-8] and photoconduction [9] properties that determine its use in a large variety of consumer products and technological applications. TiO_2 micro (MP) and nanoparticles (NP) are found in the composition of food, pharmaceutical and personal care products [10-14] (being thus ingested or having direct contact with the skin) or used as active agents (to enhance hydrophilicity or to induce bactericidal effects) in self-cleaning [15, 16] and antimicrobial technologies [17-19]. The extensive use of engineered, highly reactive, TiO_2 nanomaterials (specifically designed for particular applications) raises increasing concern regarding their potential harmful effects to humans and environment.

Irrespective of the way they enter the human body, TiO_2 nanoparticles represent exogenous substances and trigger immune responses that involve specialized immune cells, especially macrophages, which actively internalize such foreign particles [20, 21]. The phagocytic activity of macrophage cells is often associated with generation of reactive oxygen species (ROS) and inflammation [21-23]. In the case of NP exposure, these two fundamental immunological processes are interdependent, the NP-induced ROS generation leading to activation of redox-dependent pro-

inflammatory mechanisms [24, 25]. Activated macrophages play a key role in promoting and maintaining inflammation through secretion of pro-inflammatory mediators including IL-6. However, the relationship between the structural and physicochemical properties of engineered nanoparticles and their ROS generation and pro-inflammatory effects in macrophage cells remains unclear.

In this context, we have studied several *in vitro* effects of three types of TiO_2 nanoparticles on RAW 264.7 macrophages, a frequently used *in vitro* model for inflammation-related studies. The cells were exposed to Degussa P25 titania and two other types of TiO_2 nanoparticles synthesized by a hydrothermal procedure in our laboratory: undoped (HT) and Fe^{3+}-doped (FeHT).

The tested nanomaterials were such chosen to offer the possibility to investigate the relevance of semiconductor bandgap energy, specific surface area, photocatalytic efficiency and suspension stability for the results obtained in biochemical tests regarding cytotoxicity, intracellular ROS production and inflammatory processes.

The inflammation marker considered in our study was the interleukin-6 (IL-6) cytokine. IL-6 is produced at the site of inflammation by a variety of cell types but its most important sources are macrophages and monocytes [26]. IL-6 may exhibit its pro-inflammatory action by either activating its near cells (paracrine action) to produce pro-inflammatory mediators or by acting upon its source cell (autocrine action) to promote its own release through a positive feedback mechanism. Therefore, IL-6 plays a key role in propagating chronic inflammation [27, 28].

The understanding of the relationship between structural and physicochemical nanoparticle properties and the basic immune response they induce under *in vitro* and *in vivo* conditions helps researchers develop synthesis methods optimized for producing biocompatible nanomaterials.

Materials and Methods

Materials synthesis

To prepare the undoped and iron-doped TiO_2 nanoparticles, $TiCl_3$ (solution 15 % in HCl 10 %, from Merck) and Fe_2O_3 (RITVERC, 95.44 % ^{57}Fe Isotopic Enrichment) were used as starting reagents [29].

The Fe^{3+} (1 at. %)-doped TiO_2 was synthesized by coprecipitation, NH_4OH being dropwise added to a mixture of $TiCl_4$ (obtained by oxidizing $TiCl_3$ by air bubbling) and $FeCl_3$ (obtained by reacting Fe_2O_3 to hydrochloric acid (4N)). The addition of NH_4OH was stopped at pH=8. The obtained precipitate was separated by filtration and washed with deionized water. The hydrothermal treatment underwent at 200 °C, for one hour, in a 50 cm^3 Teflon-lined autoclave.

The undoped TiO_2 was synthesized in a similar manner, using the titanium precursor only.

Materials characterization

The physicochemical (structural, morphological, optical, colloidal) properties of the synthesized nanomaterials were characterized by X-ray diffraction (XRD), Mössbauer spectroscopy, transmission electron microscopy (TEM), Brunauer-Emmett-Teller (BET) nitrogen adsorption, dynamic light scattering (DLS), UV-Vis reflectance spectroscopy, diffuse reflectance infrared Fourier transform spectroscopy (DRIFT) and *energy-dispersive X-ray spectroscopy* (EDX). The detailed description of the used material characterization methods was presented in a previous paper [30].

Determination of cell viability

The RAW 264.7 macrophages were seeded in 24-well culture plates, in volumes of 1 ml of DMEM-F12 culture medium (containing 10% FBS-complete culture medium), at a density of 1 x 10^5 cells/cm^2. After 24 h of incubation (required for cell adhesion) the culture medium was removed and replaced with volumes of 1ml of fresh medium containing 1, 10, 50, 100, 200 µg of the tested TiO_2 nanoparticles (P25, HT, FeHT). After 24, 48 and 72 h respectively, the medium containing nanoparticles was discarded and volumes of 300 µl MTT solution (1 mg/ml MTT in PBS) were added to each well. The obtained samples were incubated for 2 hours at 37°C, 5% CO_2 and 90% relative humidity. The MTT solution was afterwards removed and volumes of 300 µl of DMSO (Aldrich) were added to each well in order to dissolve the formed formazan crystals. The absorbance of the purple formazan solution was determined at 540 nm using a Thermo Multiskan EX spectrophotometer.

The cell viability was expressed as percent versus control (untreated cells). Four technical replicates were used for each tested sample and a total number of three independent biological replications were conducted.

The same procedure was performed for cell samples containing TiO_2 (in the above mentioned concentrations) and 22mM Mannitol (used as ROS scavenger). Cell viability was determined as described above after 72 hours of treatment and expressed as percent versus control (untreated cells).

All results are represented as average values ± standard deviation (error bars).

Determination of intracellular ROS production

The intracellular ROS production was determined for cells treated with TiO_2 alone (1, 10, 50, 100, 200 µg TiO_2/ml of culture medium) or co-treated with TiO_2 and Mannitol (22 mM).

After 24 hours of incubation, the culture medium (containing the treating agents) was discarded and replaced with fresh medium containing DCFH-DA (0.2 µl of stock solution (2'-7'-diclorofluorescein-diacetat (DCFH-DA) 25 mg/mL in PBS) in 1 ml of culture medium).

The obtained samples were thermostat incubated for 30 minutes. After incubation, the culture medium containing DCFH-DA was discarded, the cells being detached with trypsin (0.25% trypsin and 0.53 mM EDTA solution) and suspended in PBS. The samples were centrifuged for 10 min at 1500 rpm and 4°C and the cell supernatant was removed. The cells were washed twice by centrifugation in 2 ml PBS to remove the excess of fluorescein and then resuspended in 500 µl PBS. Suspensions were homogenized and volumes of 100 µl of each sample were transferred to 96-well plates. Fluorescence signals were analysed using a Fluoroskan FL (Thermo) fluorimeter with 485 nm excitation and 530 nm emission wavelengths, respectively. Control samples, consisting of untreated cells (or cells treated with Mannitol alone), were subjected to the same procedure. Three identical samples (technical replicates) were used for each tested case and a total number of three independent biological replications were conducted. The results are expressed as percent versus control and represented as average values ± standard deviation (error bars).

Quantification of IL-6 in culture supernatants

The quantification of IL-6 in culture supernatants was performed using the Mouse IL-6 Quantikine ELISA Kit (R&D Systems).

The cultured RAW 264.7 macrophages were incubated with TiO_2 nanoparticles (P25, HT, FeHT) for 24 h. Culture supernatants were afterwards placed in ELISA plates coated with purified anti-(IL-6) antibodies (capture antibodies). The antigen (IL-6) present in each culture supernatant was bound by the capture antibody molecules. After two hours, the content of the plates was discarded and the plates were washed to remove the unbound antibody – antigen systems. A second anti-(IL-6) antibody, coupled with the horseradish peroxidase enzyme (antibody/enzyme conjugate), was added to the system to bind the antigen (which was already fixed to the bottom of the plate by the capture antibody). The content of the plates was discarded again and the plates were washed to remove all molecules that did not form *capture antibody – antigen (IL-6) – antibody/enzyme conjugate* chains. The substrate solution (1:1 mixture of stabilized hydrogen peroxide and stabilized chromogen peroxide (tetramethylbenzidine)) was subsequently added to the plates and converted to a colored compound by the bound horseradish peroxidase enzyme.

The absorbance of the colored solution was proportional to the concentration of bound enzyme and IL-6 respectively.

Control samples consisting of untreated cells were subjected to the same, above described, procedure. The concentration of IL-6 in the sample was calculated based on a standard curve obtained by performing the above described protocol using known concentrations of IL-6.

Three identical samples (technical replicates) were used for each tested case and a total number of three independent biological replications were conducted. The results are expressed as percent versus control and represented as average values ± standard deviation (error bars).

Non-cellular effects of TiO_2 nanoparticles on the fluorescence of fluorescein sodium salt

Independent volumes of 1 ml of DMEM-F12 culture medium were mixed with volumes of 1 ml of TiO_2 aqueous suspension (100 µg/ml) corresponding to each of the tested materials (P25, HT and FeHT). The obtained samples were thermostat incubated for 24 hours. After incubation, the samples were centrifuged and the supernatants were discarded. Volumes of 1 ml of fluorescein sodium salt solution were added to each tube and vortexed. All samples were thermostat incubated for 30 minutes. The samples were centrifuged again and volumes of 200 µl of clear supernatant were collected, their fluorescence being measured and compared to the fluorescence of the untreated fluorescein solution.

Data analysis and representation

Data statistical analysis and graphics were made using the SigmaPlot-11 software package. Depending on data normality, either one-way ANOVA or one-way ANOVA on ranks tests were performed, together with the *Student–Newman–Keuls* (SNK) post hoc test. Events with *p*-values < 0.05 were considered significant. Samples statistically different from controls were marked on figures with a (*).

Results

Materials characteristics

The structural and physicochemical characteristics of the three types of TiO_2 nanoparticles used in the present study were described and

discussed in detail in a previous paper [30]. Briefly, all three types of TiO_2 nanomaterials had average particle sizes between 10-30 nm (determined by TEM; HT and FeHT were smaller than Degussa P25) and similar shapes (no needle shaped particles). While the hydrothermal (HT and FeHT) samples had anatase structure, Degussa P25 TiO_2 was a mixture of anatase and rutile phases with anatase/rutile weight ratio of 85:15 (%). Specific surface areas (determined by BET nitrogen adsorption method) were 49 m^2/g for Degussa P25, 130.62 m^2/g for HT and 114.81 m^2/g for FeHT.

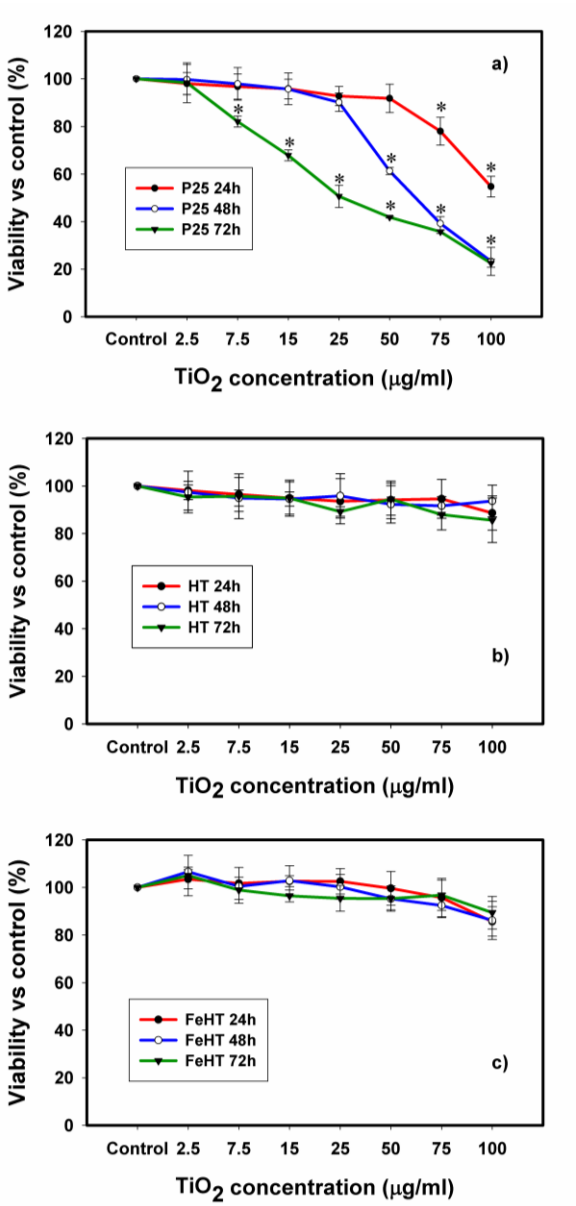

Figure 1: Viability of RAW 264.7 cells after 24, 48 and 72 h of treatment with: (a) Degussa P25, (b) HT and (c) FeHT; (*) – significant differences with respect to control ($p < 0.05$)

All three types of nanomaterials acquired similar amounts of negative surface charge (Zeta potential) when dispersed in DMEM culture medium. The hydrophilic Degussa P25 had significantly higher colloidal stability in aqueous suspension compared to HT and FeHT, this observation suggesting the hydrophobic character of the hydrothermal materials [31]. Fetal bovine serum (FBS) proteins had strong steric stabilization effects on P25 nanoparticles suspended in cell culture media, only insignificant such effects being observed for FeHT and HT. The semiconductor energy band gaps (E_g) of Degussa P25 and HT were both around 3 eV and the iron-doped sample (FeHT) had $E_g = 2.848$ eV.

Cell viability

Important viability decreases (between 11-78 %) were observed among the cells exposed to P25 nanoparticles (Fig. 1). The cell killing effect of this material was most prominent after 72 hours of treatment. In this case, significant and concentration-dependent (direct proportionality) viability reductions were obtained for TiO_2 concentrations higher than 7.5 μg/mL (Fig. 1a). For shorter treatment times (48 h and 24 h), significant viability reductions were observed, only for TiO_2 concentrations higher than 25 μg/mL in the 48 h experiment and 50 μg/mL in the 24 h experiment. The hydrothermal TiO_2 samples (HT and FeHT) showed similar behavior, inducing no significant cell killing effects within the concentration range used in this study (Fig. 1b-c).

The occurrence of photocatalytic interferences between TiO_2 and MTT [32, 33] was tested for all nanomaterials and only weak effects were observed in the case of Degussa P25 (data not shown). This aspect was considered in data analysis in a manner similar to that described by Lupu and Popescu [32].

The cytotoxic effect of Degussa P25 TiO_2 was drastically reduced in the presence of the ROS (especially HO·) scavenger. In this case, cell viability was only slightly decreased (with 11-15 % with respect to untreated cells) (Fig. 2). Mannitol alone did not significantly influence cell viability compared with negative control (untreated cells) (data not shown).

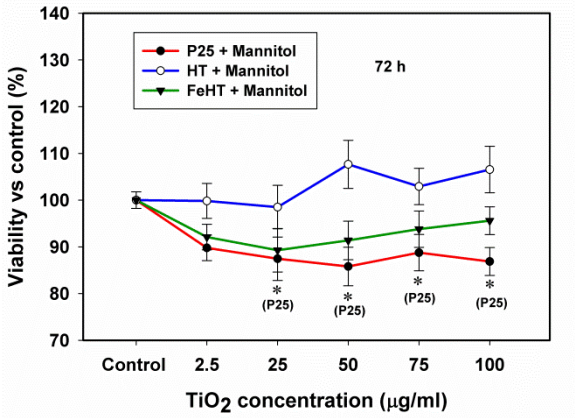

Figure 2: Viability of RAW 264.7 cells after 72 h of co-treatment with TiO_2 and Mannitol; (*) – significant differences with respect to control ($p < 0.05$)

Intracellular ROS production

The intracellular ROS production induced in macrophage cells treated with P25, HT and FeHT nanoparticles is displayed in Fig. 3a. The determined ROS production varied between 109-147% (with respect to control) and was directly proportional to the used TiO_2 concentration in all cases. All the tested nanomaterials induced significant intracellular ROS generation for concentrations higher than 25µg/ml. The effect of Degussa P25 was stronger compared to that of the hydrothermal samples (Fig. 3a). For concentrations higher than 50 µg/ml, the iron-doped titania induced slightly higher ROS production in the treated cells compared to HT.

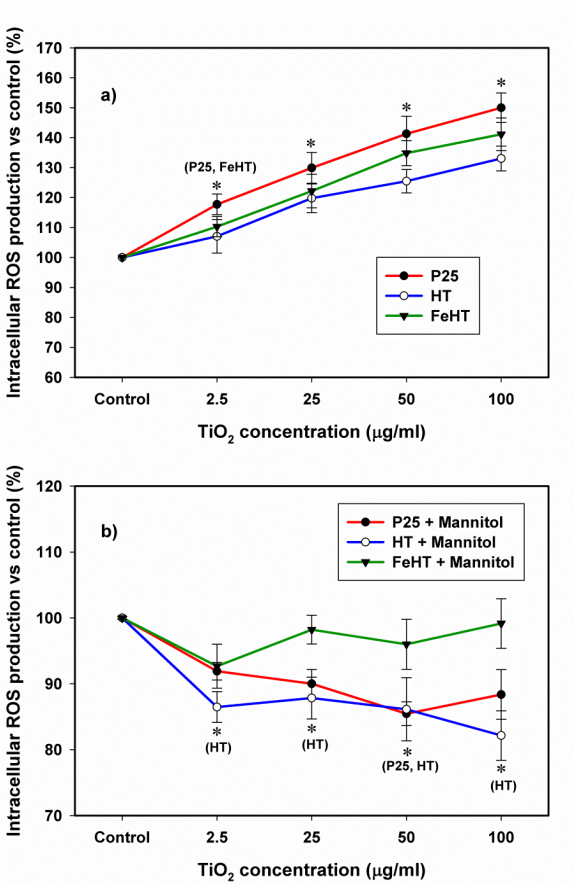

Figure 3: Intracellular ROS production in: a) RAW 264.7 cells treated with Degussa P25, HT and FeHT nanoparticles; b) RAW 264.7 cells co-treated with TiO2 and Mannitol; (*) – significant differences with respect to control ($p < 0.05$); the (*) symbols placed above particular data points refer to all materials unless otherwise specified in round brackets

In the case of co-treated cells (TiO_2 + Mannitol), the ROS scavenger had a strong effect on the intracellular ROS, the determined values being slightly lower compared to control (untreated cells) (Fig. 3b).

IL-6 release

The concentrations of interleukin-6 (IL-6) released in culture supernatants by TiO_2 stimulated RAW 264.7 macrophages are illustrated in Fig. 4. The release of the pro-inflammatory cytokine was significantly higher in Degussa P25-treated nanoparticles (increases between 15-200 % with respect to control), in a concentration-dependent (directly proportional) manner, for concentrations higher than 2.5 µg/ml. The hydrothermal nanomaterials proved to be less active in inducing the release of IL-6 by macrophages compared to Degussa P25. The iron-doped TiO_2 (FeHT) generated higher amounts of supernatant IL-6 than the undoped (HT) sample.

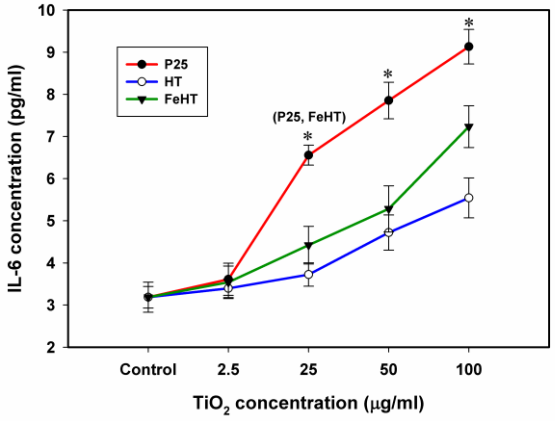

Figure 4: IL-6 release by RAW 264.7 cells treated with Degussa P25, HT and FeHT nanoparticles; (*) – significant differences with respect to control ($p < 0.05$); the (*) symbols placed above particular data points refer to all materials unless otherwise specified in round brackets

Photocatalytic effects under in vitro non-cellular conditions

The results regarding the effect of TiO_2 nanoparticles (P25, HT and FeHT) on the fluorescence of fluorescein sodium salt under *in vitro* non-cellular conditions are shown in Fig. 5.

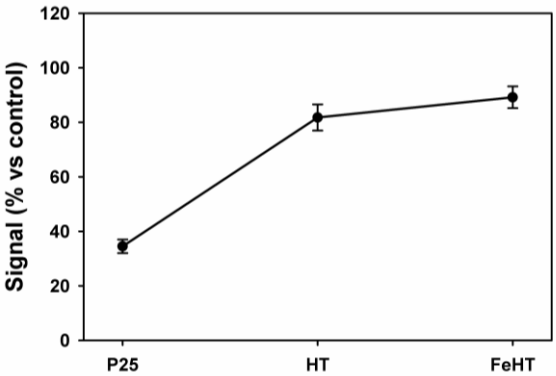

Figure 5: Decrease of fluorescence signal of fluorescein sodium salt induced by Degussa P25, HT and FeHT nanoparticles under non-cellular conditions; the control signal (untreated fluorescein sample) corresponds to 100 %

While severe reductions (on average 65% with respect to control) of the fluorescence signal

were induced by Degussa P25 nanoparticles, only weak effects were observed in the samples containing FeHT or HT. The undoped and iron-doped anatase nanoparticles led to average fluorescence reductions of 18% and 11%, respectively.

These results (qualitatively confirmed under UV irradiation at 312 nm (data not shown)), suggest a considerably higher photocatalytic ROS generation activity of the commercial TiO_2 compared to the hydrothermal samples.

Discussion

Altogether, the above described results reveal the enhanced biological reactivity (at least with respect to macrophage cells) of Degussa P25 TiO_2 compared to the hydrothermal materials (HT and FeHT).

While P25 titania shows a strong macrophage killing capacity, the HT and FeHT materials appear inert with respect to macrophage viability (Fig. 1). The observed cytotoxic effects reflect specific physicochemical characteristics of the studied TiO_2 nanomaterials that dictate their interactions with macrophage cells and their environment. Compared to the hydrophilic Degussa P25 TiO_2, the hydrothermal nanomaterials used in the present study have smaller particle sizes, higher curvature, lower surface charge in aqueous environments and similar surface charge in culture medium, as well as hydrophobic surfaces [30]. These characteristics suggest a potentially higher affinity of FeHT and HT nanoparticles for protein adsorption compared to Degussa P25 [34-40], which may contribute to the reduction of toxicity of the hydrothermal TiO_2 nanomaterials.

The severe reduction of cytotoxicity and intracellular ROS production in the cells co-treated with TiO_2 and Mannitol suggests the involvement of a ROS-mediated action mechanism of TiO_2 nanoparticles on RAW 264.7 macrophages.

Hypothetically, one triggering factor for such mechanism could be the capacity of the studied nanomaterials to photogenerate ROS on their surfaces under relevant *in vitro* conditions. Such ROS may induce membrane damage and trigger production of intracellular ROS followed by subsequent cellular processes [41, 42]

Our results clearly showed that Degussa P25 TiO_2 generated significantly higher levels of ROS compared to FeHT and HT under non-cellular conditions (Fig. 5). Although the Fe^{3+}-doped TiO_2 had a reduced energy bandgap (resulting in enhanced charge carrier photogeneration under visible light conditions) compared to the other two samples, this characteristic was not sufficient to confer higher reactivity to this nanomaterial. The reason for this is the dependency of the photocatalytic process on other factors such as charge recombination rates (influenced by the amount and localization of Fe^{3+} ions into the host TiO_2 matrix [43]) and specific physicochemical characteristics of the semiconductor-liquid interface.

Despite the known occurrence of TiO_2 induced photocatalytic processes under *in vitro* non-cellular conditions [32, 33] and the observed correlation between the *in vitro* activity of P25 TiO_2 and its non-cellular ROS generation capacity (Fig. 5), the present data is not sufficient to discuss the involvement of a macrophage activation and killing mechanism triggered by photocatalytic processes. This hypothesis remains to be further investigated.

Regarding IL-6 production, many recent studies have identified concentrations of hundreds of pg/ml IL-6 for activated macrophages [44 - 48]. In this context, although we obtained significant differences between treated cells and control in the case of P25, the very low concentrations of IL-6 corresponding to all the samples tested in our study have no biological relevance. Thus, we can't conclude that P25, HT or FeHT influenced the pro-inflammatory IL-6 production.

Summarizing, our study suggests that TiO_2 nanoparticles with hydrophilic surfaces, high surface charge and enhanced photocatalytic properties may preferentially induce macrophage cell activation and damage compared to other TiO_2 nanomaterials. The present findings help in establishing biocompatibility criteria for TiO_2 nanomaterials.

In conclusion, the conducted study has revealed relevant information regarding the generation of intracellular ROS, inflammation and cytotoxicity in macrophage cell cultures exposed to TiO_2 nanoparticles with known physicochemical properties. The undoped and Fe^{3+}-doped TiO_2 nanoparticles synthesized by a hydrothermal procedure in our laboratory exhibited reduced pro-oxidative and pro-inflammatory effects and low cytotoxicity compared to the commercial hydrophilic Degussa P25 photocatalyst. The enhanced biocompatibility of the hydrothermal TiO_2 materials was supported by their specific characteristics (particle size, surface curvature, surface charge, hydrophobicity) and reduced capacity to generate ROS under non-cellular conditions. The hydrothermal method can thus be employed to synthesize low toxicity TiO_2 nanomaterials.

Acknowledgements

Author Popescu T acknowledges funding from Romanian National Authority for Scientific Research, under Core Project PN09-450103 and from MEN-

UEFISCDI under national grants PN-II-PT-PCCA-2013-4-0419 (CLEANTEX) and PN-II-PT-PCCA-2013-4-0864(CLEANPHOTOCOAT). Author Lupu AR acknowledges support under PN-II-PT-PCCA-2013-4-1386 (NANOPATCH) national grant.

References

1. Linsebigler AL, Lu G, Yates JT Jr.Photocatalysis on TiOn Surfaces: Principles, Mechanisms and Selected Results. Chem Rev. 1995;95:735-758. http://dx.doi.org/10.1021/cr00035a013

2. Fujishima A,Rao TN, Tryk DA.Titanium dioxide photocatalysis. Journal of Photochemistry and Photobiology C: Photochemistry Reviews. 2000;1:1-21. http://dx.doi.org/10.1016/S1389-5567(00)00002-2

3. Carp O, Huisman CL,Reller A. Photoinduced reactivity of titanium dioxide. Progress in Solid State Chemistry. 2004;32:33-177. http://dx.doi.org/10.1016/j.progsolidstchem.2004.08.001

4. Son HS, Lee SJ, Cho IH,Zoh KD.Kinetics and mechanism of TNT degradation in TiO2photocatalysis. Chemosphere. 2004;57(4):309-317. http://dx.doi.org/10.1016/j.chemosphere.2004.05.008 PMid:15312729

5. Hashimoto K,Irie H,Fujishima A. TiO2Photocatalysis: A Historical Overview and Future Prospects. Japanese Journal of Applied Physics. 2005; 44(12):8269-8285. http://dx.doi.org/10.1143/JJAP.44.8269

6. Chen X, Mao SS.Titanium Dioxide Nanomaterials: Synthesis, Properties, Modifications and Applications. Chem Rev. 2007;107(7):2891–2959. http://dx.doi.org/10.1021/cr0500535 PMid:17590053

7. Kumar SG, Devi LG.Review on Modified TiO2Photocatalysis under UV/Visible Light: Selected Results and Related Mechanisms on Interfacial Charge Carrier Transfer Dynamics. J Phys Chem A. 2011;115(46):13211–13241. http://dx.doi.org/10.1021/jp204364a PMid:21919459

8. Pap Z, Radu A, Hidi IJ, et al.Behavior of gold nanoparticles in a titania aerogel matrix: photocatalytic activity assessment and structure investigations. Chinese Journal of Catalysis. 2013;34:734–740. http://dx.doi.org/10.1016/S1872-2067(11)60500-7

9. Chen RS, Chen CA, Tsai HY, Wang WC, Huang YS. Photoconduction Properties in Single-Crystalline Titanium Dioxide Nanorods with Ultrahigh Normalized Gain. J Phys Chem C. 2012; 116(6):4267–4272. http://dx.doi.org/10.1021/jp209999j

10. Meena R, Pal R, Pradhan SN, Rani M, Paulraj R. Comparative study of TiO2 and TiSiO4 nanoparticles induced oxidative stress and apoptosis of HEK-293 cells. Adv Mat Lett. 2012;3(6):459-465.

11. Rowe RC, Sheskey PJ, Quinn ME. Handbook of Pharmaceutical Excipients. Sixth Ed. Pharmaceutical Press and American Pharmacists Association, 2009.

12. Contado C,Pagnoni A. TiO2nano- and micro-particles in commercial foundation creams: Field Flow-Fractionation techniques together with ICP-AES and SQW Voltammetry for their characterization. Analytical Methods. 2010;2(8):1112-1124. http://dx.doi.org/10.1039/c0ay00205d

13. Lorenz C, Tiede K, Tear S, Boxall A, von Goetz N, Hungerbuhler K. Imaging and Characterization of Engineered Nanoparticles in Sunscreens by Electron Microscopy, Under Wet and Dry Conditions.International Journal of Occupational and Environmental Health. 2010;16(4):406-428. http://dx.doi.org/10.1179/oeh.2010.16.4.406 PMid:21222385

14. Scotter MJ. Methods for the determination of European Union-permitted added natural colours in foods: a review. Food Additives and Contaminants Part A-Chemistry Analysis Control Exposure & Risk Assessment. 2011; 28(5):527-596. http://dx.doi.org/10.1080/19440049.2011.555844 PMid:21424961

15. Diamanti MV, Ormellese M, Pedeferri MP. Characterization of photocatalytic and superhydrophilic properties of mortars containing titanium dioxide. Cement and Concrete Research. 2008;38(11):1349–1353. http://dx.doi.org/10.1016/j.cemconres.2008.07.003

16. Quagliarini E, Bondioli F, Goffredo G-B, Cordoni C, Munafò P. Self-cleaning and de-polluting stone surfaces: TiO2 nanoparticles for limestone. Construction and Building Materials. 2012;37:51–57. http://dx.doi.org/10.1016/j.conbuildmat.2012.07.006

17. Herrera Melián JA, Do-a Rodrígue JM, Viera Suárez A, et al. The photocatalytic disinfection of urban waste waters. Chemosphere. 2000;41(3):323–327. http://dx.doi.org/10.1016/S0045-6535(99)00502-0

18. Fu G, Vary PS, Lin C-T. Anatase TiO2 Nanocomposites for Antimicrobial Coatings. J Phys Chem B. 2005;109(18):8889-8898. http://dx.doi.org/10.1021/jp0502196 PMid:16852057

19. Chung CJ, Lin HI, Tsou HK, Shi ZY, He JL.An antimicrobial TiO2 coating for reducing hospital-acquired infection. J Biomed Mater Res B: Appl Biomater. 2008;85(1):220-224. http://dx.doi.org/10.1002/jbm.b.30939 PMid:17854067

20. Skoczen SL, Potter TM, Dobrovolskaia MA. In vitro analysis of nanoparticle uptake by macrophages using chemiluminescence. Methods Mol Biol. 2011;697:255-261. http://dx.doi.org/10.1007/978-1-60327-198-1_27 PMid:21116975

21. Weissleder R, Nahrendorf M, Pittet MJ. Imaging macrophages with nanoparticles. Nature Materials. 2014;13:125–138. http://dx.doi.org/10.1038/nmat3780 PMid:24452356

22. Forman HJ, Torres M. Redox signaling in macrophages. Molecular Aspects of Medicine. 2001;22(4–5):189–216. http://dx.doi.org/10.1016/S0098-2997(01)00010-3

23. Kusaka T, Nakayama M, Nakamura K, Ishimiya M, Furusawa E, Ogasawara K. Effect of Silica Particle Size on Macrophage Inflammatory Responses.PLoS ONE. 2014; 9(3): e92634. http://dx.doi.org/10.1371/journal.pone.0092634 PMid:24681489 PMCid:PMC3969333

24. Manke A, Wang L, Rojanasakul Y.Mechanisms of Nanoparticle-Induced Oxidative Stress and Toxicity. BioMed Research International. 2013; Article ID 942916.

25. Kim J-H, Jang A-S, Shin EK, et al. Particle-induced expression of SF20/IL25 is mediated by reactive oxygen species and NF-κB in alveolar macrophages. Mol Cell Toxicol. 2010;6:305-312. http://dx.doi.org/10.1007/s13273-010-0041-2

26. Akdis M, Burgler S, Crameri R, et al. Interleukins, from 1 to 37, and interferon-g: Receptors, functions, and roles in diseases. J Allergy ClinImmunol. 2011;127(3):701-721. http://dx.doi.org/10.1016/j.jaci.2010.11.050 PMid:21377040

27. Barnes TC, Anderson ME, Moots RJ. TheMany Faces of Interleukin-6: The Role of IL-6 in Inflammation, Vasculopathy and Fibrosis in Systemic Sclerosis. International Journal of Rheumatology. 2011; Article ID 721608. http://dx.doi.org/10.1155/2011/721608 PMid:21941555 PMCid:PMC3176444

28. Gabay C. Interleukin-6 and chronic inflammation. Arthritis Res Ther. 2006;8(Suppl 2):S3. http://dx.doi.org/10.1186/ar1917 PMid:16899107 PMCid:PMC3226076

29. Diamandescu L, Vasiliu F, Tarabasanu-Mihaila D, et al. Structural and photocatalytic properties of iron-and europium-doped TiO2 nanoparticles obtained under hydrothermal conditions. Mater Chem Phys. 2008;112(1):146–153. http://dx.doi.org/10.1016/j.matchemphys.2008.05.023

30. Popescu T, Lupu AR, Diamandescu L, et al. Effects of TiO2 nanoparticles on the NO2- levels in cell culture media analyzed by Griess colorimetric methods. Journal of Nanoparticle Research. 2013;15: 1449-1466. http://dx.doi.org/10.1007/s11051-013-1449-0

31. Ding X, An T, Li G, et al. Preparation and characterization of hydrophobic TiO2 pillared clay: the effect of acid hydrolysis catalyst and doped Pt amount on photocatalytic activity. J Colloid Interface

Sci. 2008; 320:501–507. http://dx.doi.org/10.1016/j.jcis.2007.12.042 PMid:18279880

32. Lupu AR, Popescu T. The noncellular reduction of the MTT tetrazolium salt by TiO2 nanoparticles and its implications for cytotoxicity assays. Toxicol In Vitro. 2013;27(5):1445–1450. http://dx.doi.org/10.1016/j.tiv.2013.03.006 PMid:23531555

33. Popescu T, Lupu AR, Raditoiu V, Purcar V, Teodorescu VS. On the photocatalytic reduction of MTT tetrazolium salt on the surface of TiO2 nanoparticles: Formazan production kinetics and mechanism. J Colloid Interface Sci. 2015;457:108-120. http://dx.doi.org/10.1016/j.jcis.2015.07.005 PMid:26164242

34. Rahman M, Laurent S, Tawil N, Yahia L, Mahmoudi M. Protein-Nanoparticle interactions. The Bio-Nano Interface. Springer-Verlag Berlin Heidelberg. 2013. http://dx.doi.org/10.1007/978-3-642-37555-2

35. Lynch I, Dawson KA. Protein-nanoparticle interactions. Nano Today. 2008;3:40-47. http://dx.doi.org/10.1016/S1748-0132(08)70014-8

36. Lundqvist M, Stigler J, Cedervall T, et al. The evolution of the protein corona around nanoparticles: a test study. ACS Nano. 2011;5:7503-7509. http://dx.doi.org/10.1021/nn202458g PMid:21861491

37. Mahmoudi M, Lynch I, Ejtehadi MR, Monopoli MP, Bombelli FB, Laurent S. Protein-nanoparticle interactions: opportunities and challenges. Chem Rev. 2011;111:5610-5637. http://dx.doi.org/10.1021/cr100440g PMid:21688848

38. Aggarwal P, Hall JB, McLeland CB, Dobrovolskaia MA, McNeil SE. Nanoparticle interaction with plasma proteins as it relates to particle biodistribution, biocompatibility and therapeutic efficacy. Adv Drug Deliv Rev. 2009;61:428-437. http://dx.doi.org/10.1016/j.addr.2009.03.009 PMid:19376175 PMCid:PMC3683962

39. Gessner A, Waicz R, Lieske A, Paulke BR, Mader K, Muller RH. Nanoparticles with decreasing surface hydrophobicities: influence on plasma protein adsorbtion. Int J Pharm. 2000;196:245-249. http://dx.doi.org/10.1016/S0378-5173(99)00432-9

40. Cedervall T, Lynch I, Lindman S, et al. Understanding the nanoparticle-protein corona using methods to quantify exchange rates and affinities of proteins for nanoparticles. Proc Natl Acad Sci USA. 2007;104:2050-2055. http://dx.doi.org/10.1073/pnas.0608582104 PMid:17267609 PMCid:PMC1892985

41. Wang J, Fan Y. Lung Injury Induced by TiO2 Nanoparticles Depends on Their Structural Features: Size, Shape, Crystal Phases and Surface Coating. Int J Mol Sci. 2014;15:22258-22278. http://dx.doi.org/10.3390/ijms151222258 PMid:25479073 PMCid:PMC4284706

42. Stark G. Functional consequences of oxidative membrane damage. J Membr Biol. 2005;205(1):1-16. http://dx.doi.org/10.1007/s00232-005-0753-8 PMid:16245038

43. Othman SH, Rashid SA, Ghazi TIM, Abdullah N. Fe-Doped TiO2 nanoparticles produced via MOCVD: synthesis, characterization, and photocatalytic activity. J Nanomater. 2011; Article ID 571601. http://dx.doi.org/10.1155/2011/571601

44. Chen B-C, Liao C-C, Hsu M-J, Liao Y-T, Lin C-C, Sheu J-R, Lin C-H. Peptidoglycan-induced IL-6 Production in Raw264.7 Macrophages is Mediated by Cyclooxygenase-2, PGE2/PGE4 Receptors, Protein Kinase A, IkB Kinase and NF-kB. The Journal of Immunology. 2006;177:681-693. http://dx.doi.org/10.4049/jimmunol.177.1.681

45. Sormou LW, Zhang Z, Li R, Chen N, Guo W, Huo M, Guan S, Lu J, Deng X. Regulation of Inflammatory Cytokines in Lipopolysaccharide Stimulated RAW 264.7 Murine Macrophage by 7-O-Methyl-narigenin. Molecules. 2012;17:3574-3585. http://dx.doi.org/10.3390/molecules17033574 PMid:22441335

46. Wang H, Cao Z-R. Anti-Inflammatory Effects of (-)-Epicatechin in Lipopolysaccharide-stimulated RAW 264.7 Macrophages. Tropical Journal of Pharmaceutical Research. 2014;13(9):1415-1419

47. Lee A-J, Cho K-J, Kim J-H. MyD88 – BLT2 – dependent cascade contributes to LPS-induced interleukin-6 production in mouse macrophage. Experimental & Molecular Medicine. 2015;47:e156. http://dx.doi.org/10.1038/emm.2015.8 PMid:25838003

48. Ji G, Zhang Y, Yang Q, Cheng S, Hao J, Zhao X, Jiang Z. Genistein Suppresses LPS-Induced Inflammatory Response through inhibiting NF-kB following AMP Kinase Activation in RAW 264.7 Macrophages. PLoS ONE. 2012;7(12): e53101. http://dx.doi.org/10.1371/journal.pone.0053101 PMid:23300870 PMCid:PMC3534028